body of revolution, far from the axis," Proc. Roy. Soc. (London) A201, 89–109 (March 1950).

[8] Hubbard, H. H., Maglieri, D. J., Huckel, V., and Hilton, D. A. (with appendix by H. W. Carlson), "Ground measurements of sonic-boom pressures for the altitude range of 10,000 to 75,000 feet," NASA TR R-198 (1964). (Supersedes NASA TM X-633.)

[9] Walkden, F., "The shock pattern of a wing-body combination, far from the flight path," Aeronaut. Quart. IX, Pt. 2, 164–194 (May 1958).

[10] Whitham, G. B., "The flow pattern of a supersonic projectile," Commun. Pure Appl. Math. V, 301–348 (August 1952).

[11] Middleton, W. D. and Carlson, H. W., "A numerical method for calculating near-field sonic-boom pressure signatures," NASA TN D-3082 (1965).

[12] Carlson, H. W., Mack, R. J., and Morris, O. A., "Sonic-boom pressure-field estimation techniques," J. Acoust. Soc. Am. (submitted for publication).

[13] McLean, F. E. and Shrout, B. L., "Design methods for minimization of sonic-boom pressure-field disturbances," J. Acoust. Soc. Am. (submitted for publication).

MAY-JUNE 1967 J. AIRCRAFT VOL. 4, NO. 3

Limits on Minimum-Speed V/STOL Wind-Tunnel Tests

WILLIAM H. RAE JR.*
University of Washington, Seattle, Wash.

This paper presents the results of a systematic series of wind-tunnel tests, which have determined the maximum size rotor that can be tested in closed-throat wind tunnels both as a function of the downwash angle and as a function of tunnel geometry. For a given size rotor and tunnel there appears to be a maximum value of downwash that can be tolerated. If this value of downwash is exceeded, the flow through the wind tunnel is no longer similar to the flow that would be encountered in free flight but rather represents a flow similar to recirculation. The point at which the maximum downwash is reached is called the flow breakdown point. Similar results have also been obtained using jet flaps and jet-lift models. It is also shown that this flow breakdown is a function of tunnel geometry and that the allowable downwash angles are different for rectangular tunnels with width-to-height ratios of W/H = 1.50, 1.00, 0.67, and 0.50. The addition of fillets to the test section is also shown to have an adverse effect on the allowable downwash angle. At the present time, the optimum tunnel configuration for rotors and other types of V/STOL vehicles is not known.

Nomenclature

A_m = momentum area of lifting system
A_T = cross-sectional area of wind tunnel
C = cross-sectional area of wind tunnel
C_L = coefficient of lift L/qS
H = height of wind tunnel
L = lift
q = dynamic pressure
R = rotor radius
S = wing area
V = velocity
W = width of wind tunnel
α = angle of attack
δ = wind-tunnel or jet boundary correction factor
θ_n = momentum downwash angle or wake deflection angle measured from horizontal axis
μ = advance ratio or tip speed ratio $V/\Omega R$
Ω = rotor angular velocity

Introduction

IN June 1963, the University of Washington started a research program supported by the Engineering Sciences Division of the U. S. Army Research Office Durham, Durham, N. C., to study operational and testing problems that might be encountered in testing V/STOL type of aircraft in wind tunnels.

The testing of V/STOL models in wind tunnels presents many problems that are very different from those encountered in the testing of conventional-type aircraft where the testing techniques are relatively well understood. One of the basic differences between the two types of aircraft is, of course, the method of generating lift. A conventional aircraft obtains its lift from a wing or wings which may be characterized by moderate values of lift coefficients and relatively low angles of downwash in the flow behind the wings. A V/STOL vehicle, on the other hand, at speeds near transition flight, has large values of lift coefficients and downwash angles that vary from 90° at hover to 3°–6° at high forward speed. This large wake deflection angle with high energy added to it appears to present one of the most difficult problems that is encountered in wind-tunnel testing of V/STOL type of vehicles.

In an attempt to gain an insight into the problems of testing V/STOL type vehicles in a wind tunnel, a series of tests were run using as a vehicle a helicopter rotor. No attempt was made, however, to duplicate any specific type of rotor, but, rather, the rotor was only considered as a source of downwash. In these tests two rotors were used: 1) a four-bladed, 38-in.-diam rotor with articulated blades and 2) a three-bladed rotor with a 24-in. diam. These rotors were tested at identical operating conditions in the main 8- × 12-ft test section of the University of Washington wind tunnel and in inserts set inside the main test section.

The inserts are plywood boxes open on the ends in the direction of the wind stream and are used to simulate the ceiling, floor, and walls of wind-tunnel test sections of various geometries. The 38-in. rotor was tested at a nominal disk loading of approximately 4 psf and the 24-in. rotor at nominal disk loadings of approximately 4, 7, and 10 psf. The disk loading is defined as the lift of the rotor divided by the swept area of the rotor or the rotor disk area. Both rotors were tested at a

Presented as Preprint 66-736 at the AIAA Aerodynamic Testing Conference, Los Angeles, Calif., September 21–23, 1966; submitted September 30, 1966; revision received January 31, 1967. This work was sponsored by the Army Research Office, Durham under Grant DA-ARO(D)-31-124-G481. [3.01]

* Assistant Professor, Department of Aeronautics and Astronautics. Member AIAA.

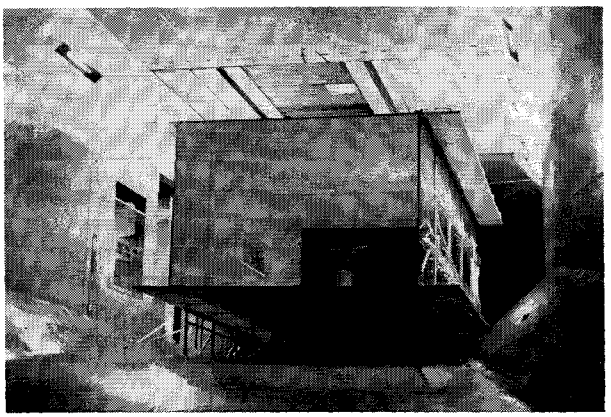

Fig. 1 24-in.-diam rotor and the 4- × 6-ft insert in the main UWAL 8 × 12 test section.

constant collective pitch or blade angle. Thus, the disk loadings were not held constant but were allowed to vary with shaft angle of attack and rotor tip speed ratio. Therefore, the values given are nominal or average values of the disk loading. Testing in this manner does not duplicate the actual flight of a helicopter. However, it is a convenient method of conducting the wind-tunnel tests and was used. Thus, it was possible to obtain data at a 4-psf disk loading with two diameters to see the effect of rotor diameter and at three disk loadings with the smaller rotor to obtain the effect of disk loading. Figure 1 shows the general arrangement of the 4- × 6-ft insert with a rotor within the 8- × 12-ft test section of the University of Washington Aeronautical Laboratory (UWAL) wind tunnel.[1,2]

Test Procedures

The flow through the inserts was calibrated in terms of the dynamic pressure and upflow. The walls of the inserts were tapered to maintain a constant static pressure within the inserts. In each insert or test section the 38-in.-diam rotor was tested at a nominal disk loading of 4 psf, and the 24-in.-diam rotor was tested with at least two disk loadings, usually the nominal 4- and 7-psf loadings.

The test procedure that was used for each rotor is as follows: A tip speed ratio sweep run was made from $\mu = 0.05$ to 0.20 at a shaft angle of $-3°$ in increments of $\Delta\mu = 0.01$ to 0.02 in the region where it was suspected that the flow had broken down. Larger increments of μ were used outside of the flow breakdown regions. Tip speed ratio, μ, for these tests is defined as the ratio of the tunnel airspeed to tip speed of the rotor. The tip speed ratio was varied by changing the tunnel speed while holding a constant rotor rpm. Then, to study the effect of the flow breakdown on wall corrections, runs were made over an angle-of-attack range of $\pm 7°$ at selected tip speed ratios on both sides of the flow breakdown point.

In addition to the rotor forces, tuft study runs showing the flow on the wall and floor were made using the 24-in. rotor at $-3°$ shaft angle for the same tip speed ratios as the tip speed ratio sweep runs for the force data. The static pressures along the tunnel walls were also recorded for all tip speed ratios at a shaft angle of $-3°$ for all rotors tested.

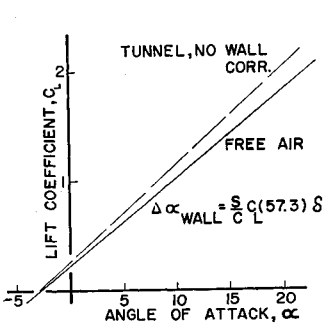

Fig. 2 Effect of tunnel wall constraints on lift curve.

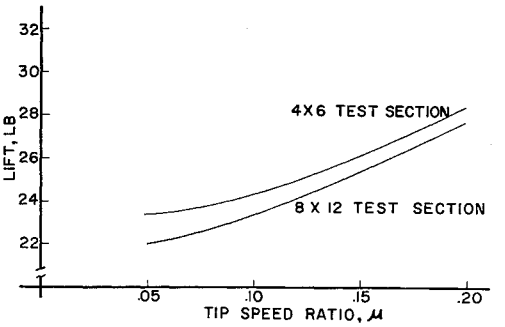

Fig. 3 Expected variation of rotor lift for different size wind tunnels.

Data Analysis

In general, if one looks at data from a wind tunnel without applying wall corrections, one obtains curves similar to those shown in Fig. 2. The effect of the wall constraints is to decrease the angle of attack at a constant value of lift coefficient. Then, to correct the tunnel data to free air (no wall effects) in the simplest case, one can apply the standard wind-tunnel wall corrections after the work of Prandtl and Glauert. This correction takes the form of $\Delta\alpha_{wall}° = \delta S/CC_L$ (57.3) where δ is the wall correction factor which is a function of model span, tunnel size, tunnel geometric configuration, and the span load of the wing; S is the model wing area; and C is the cross-sectional area of the tunnel. This equation is for a lifting system that obtains its lift from circulation. There are similar types of correction equations for vehicles with very high lifts as outlined by H. H. Heyson in Refs. 3 and 4. These equations reduce to Glauert and Prandtl's results for the case of a wing. If the wall correction equation is applied, the curve for the tunnel will be superimposed on the curve for the free air case.

Now, using the curves of Fig. 2 and considering the rotor as equivalent to a round wing at a constant angle of attack (and operating at or near a constant disk loading), curves similar to those in Fig. 3 would be obtained when going either from free air to a wind tunnel or from a large to a smaller tunnel of the same geometry. If the rotor is operated at constant rpm, then to decrease the tip speed ratio the tunnel speed is decreased; and hence the tunnel dyamic pressure is decreased. Thus, for a constant or near constant disk loading, the lift coefficient varies as the reciprocal of the tip speed ratio squared. Then, from Fig. 2, for a constant angle of attack, the ΔC_L or lift between the free air and wind-tunnel curve will increase with an increase in C_L or decreasing tip speed ratio for a rotor. Thus, the two curves on Fig. 3 are close together at high tip speed ratios (low C_L's), and at low tip speed ratios (high C_L's) the curves diverge as shown.

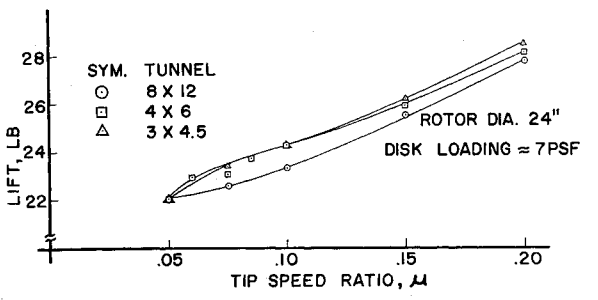

Fig. 4 Actual variation of rotor lift for different size wind tunnels.

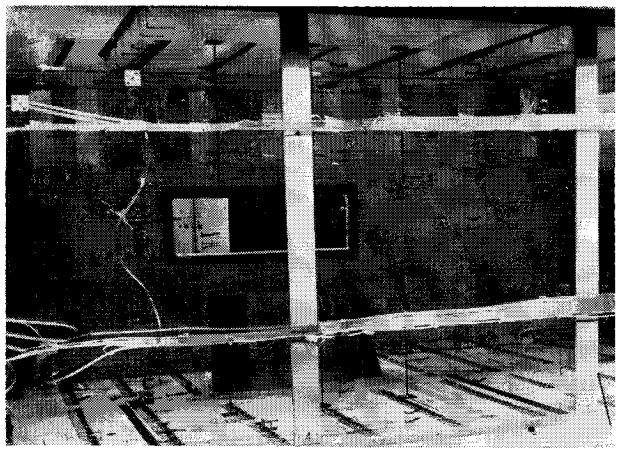

Fig. 5 Tuft studies in the 4- × 6-ft insert; tip speed ratio = 0.10, disk loading = 4.44 psf.

When a given rotor, i.e., same diameter and disk loading, was tested in the 8- × 12-ft main test section and in the 4- × 6- and 3- × 4.5-ft inserts, the results shown in Fig. 4 were obtained. These data are for the 24-in. rotor at a nominal disk loading of 7 psf. Since the data were all taken at the same rotor rpm and tunnel velocity, the discrepancy in the data between what was expected (Fig. 3) and obtained (Fig. 4) at low tip speed ratios could not be conveniently explained by Reynolds or Mach number effect, as they were constant at any given tip speed ratio. Thus, being deprived of this favorite explanation for data discrepancy, one was forced to look for another explanation. The reason for this discrepancy in the data was quite obvious when a tuft study was made of the flow through the tunnel or inserts.

These tuft studies were most enlightening, as they showed the flow pattern from the rotor's wake on the tunnel floor and walls. At moderate values of the tip speed ratio near 0.10, the flow on the floor aft of the rotor was toward the wall. This flow proceeded up the wall and aft toward the exit of the test section. As the tip speed ratio was decreased, this flow up the wall moved forward along the wall until it was opposite the rotor. As the tip speed ratio was then further reduced, the flow up the wall moved ahead of the rotor and on the advancing side of the rotor disk, a region of reversed flow developed near the tunnel floor. This region of reversed flow can extend to between $1\frac{1}{2}$ and 2 diam forward of the rotor. Figures 5 and 6 are photographs of the tufts in the 4- × 6-ft insert with the 24-in. rotor operating at tip speed ratios of 0.10 and 0.05. From these figures one can see the vertical flow up the insert wall ahead of the rotor (on either side of brace A for Fig. 6). The photo at $\mu = 0.10$ is above the flow

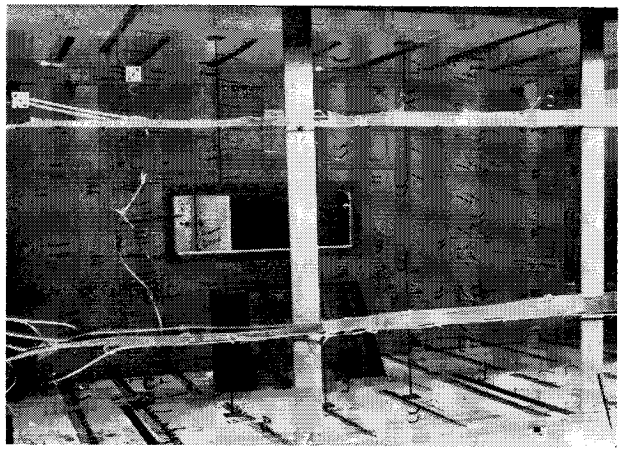

Fig. 6 Tuft studies in the 4- × 6-ft insert; tip speed ratio = 0.05, disk loading = 4.17 psf.

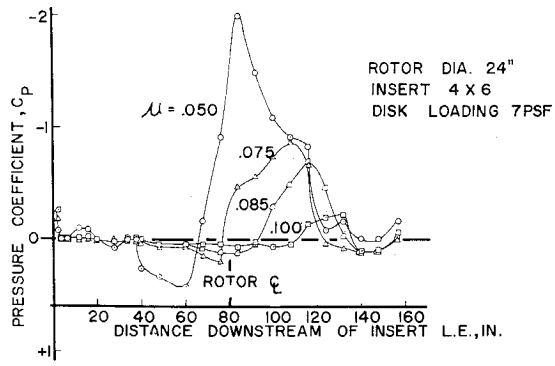

Fig. 7 Variation of pressure coefficient along wall under advancing blade.

breakdown point, and the photo at $\mu = 0.05$ is below the break down point. The flow breakdown in this case was at $\mu = 0.06$. The cross flow on the floor can be seen on Fig. 6 by the row of tufts near the trailing edge of the fairing that houses the rotor drive system.

The variation of the static pressure along the tunnel wall under the advancing blade in the form of pressure coefficient vs tunnel station is shown in Fig. 7. For this tunnel and rotor the flow breakdown occurred at a tip speed ratio of 0.079. From this plot the effect of the flow breakdown on the tunnel wall static pressures can be seen. At the tip speed ratio of $\mu = 0.10$ (above breakdown), the static pressure is constant in the region of the rotor. As the tip speed is reduced and the flow begins to break down, the effect on the wall statics in the region of the rotor can be seen. Note also how the flow breakdown spreads forward past the rotor as the tip speed ratio is reduced.

Results

From analysis of plots similar to Figs. 4 and 7, plus tuft photographs, a limit curve for testing rotors in closed tunnels was developed. These results are shown on Figs. 8 and 9. Figure 8 shows an estimated limit curve for model area to tunnel cross-sectional area as a function of rotor momentum downwash as calculated from Refs. 3 or 5. The curves on Fig. 8 show the maximum-size model for a rectangular wind tunnel with a width-to-height ratio of 1.5. Also, the effect of fillets is shown which, for the size of fillets tested, reduced the allowable downwash or the maximum lift of the model. These curves indicate that for testing in the transition region of a V/STOL aircraft, where large downwash angles are desired, one must use a small value of A_m/A_T. The curves also indicate that it is desirable to use a wind tunnel without corner fillets, as the addition of large fillets reduces the allowable model size by approximately 22% for 30° of downwash.

The next figure (Fig. 9) shows the effect of changing the geometry of the wind tunnel. These results show that a rec-

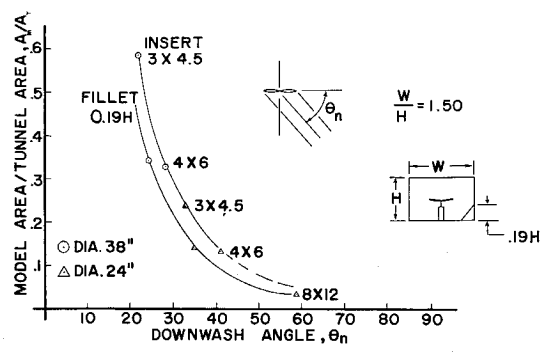

Fig. 8 Estimated limit of rotor downwash angle for rectangular tunnel with and without fillets.

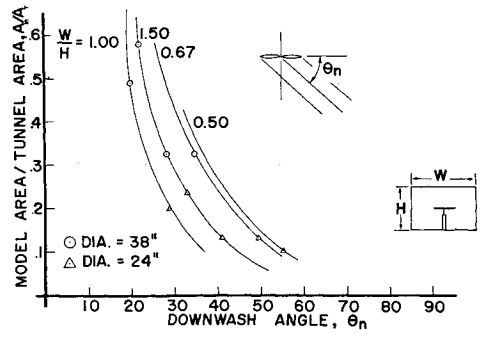

Fig. 9 Estimated limit of rotor downwash angle for various rectangular wind tunnels.

tangular tunnel $W/H = 1.5$ or $W/H = 0.67$ is superior to a square tunnel $W/H = 1.0$ for a given ratio of model to tunnel size. This can be seen on Fig. 10, which is a cross plot of Fig. 9 for a model to tunnel size ratio $A_m/A_T = 0.20$. Thus, for a fixed A_m/A_T the rectangular tunnels allow one to test further into the transition region than a square tunnel. The addition of fillets to any of the tunnels shown on Fig. 9 will reduce the allowable downwash as shown on Fig. 8. It is assumed that a round tunnel would be the worst configuration of all, as the flow breakdown does not affect the data until the flow starts up the walls of the tunnel near the rotor; and, of course, the round tunnel or one with large fillets would make it easier for the wake to flow up the tunnel walls.

It should be noted that the results given on Fig. 8 are given as a function of the rotor's momentum downwash angle. Data taken in the 3- × 4.5- ft and 4- × 6-ft inserts using the 24-in.-diam rotor at three nominal disk loadings (4, 7, and 10 psf) gave a flow breakdown point at different tunnel speeds and, hence, different tip speed ratios. The momentum downwash angles were, however, identical at the flow breakdown point. Thus, the flow breakdown is a function of the momentum downwash angle only and not a function of the disk loading and airspeed, which merely determine the downwash angle.

Discussion

No theoretical treatment is presently available because the phenomenon being studied is the degree to which the flow actually deviates from the model that is generally assumed in theoretical studies. Although certain physical explanations are offered for the phenomenon, all of the data results are from experimental measurements. Thus, no assumptions of doubtful validity are required, as would be the case in a theoretical treatment. The data presented herein are directly applicable only to single rotors or lifting propellers. However results of tests from different facilities using such wildly divergent models as jet flaps and tilt wings indicate that the results and the approximate numerical values obtained can be applied to that class of V/STOL vehicles that have their powered lift system distributed across the span.

The results shown on Fig. 9 could be used to determine the most desirable tunnel configuration in which to conduct a test. Assuming that the vehicle weight and, hence, its lift is known, as well as the desired velocity in the transition region, the required value of momentum downwash θ_n can be determined. Then for this value of θ_n, variation of A_m/A_T with W/H can be found from Fig. 9. This type of cross plot is shown on Fig. 11 for a value of θ_n of 30°. Now, assuming that there are two wind tunnels available, one a square tunnel $W/H = 1.0$ and the other a rectangular tunnel $W/H = 1.5$ and $W/H = 0.67$ (both tunnels having the same area of 400 ft²), it can be seen from Fig. 11 that for a constant A_T the allowable model size will vary for a fixed value of θ_n.

Figure 11 shows that the narrow, deep tunnel $W/H = 0.67$ has the largest value of A_m/A_T and, hence, the largest model. However, this result tends to be misleading, as shown on Fig. 12, which shows a sketch of the tunnels and models. As can be seen, the narrow, deep tunnel with the largest A_m/A_T has a rotor whose diameter is equal to 90% of the tunnel width. The data used for the $W/H = 0.67$ tunnel on Figs. 11 and 12 were extrapolated from the curve on Fig. 9, where maximum diameter to tunnel width ratio used for the 0.67 tunnel was 0.79. It is possible that a model spanning 90% of this tunnel may encounter flow breakdown at a downwash angle slightly different than the 30° used as an example. It is obvious that using such a large model will give a large degree of nonuniformity of interference over the region of the model. This problem is discussed in some detail in Ref. 3. Thus, the narrow, deep tunnel does not seem to be as desirable as it first appeared because of the flow distortion around the model due to the proximity of the tunnel walls. On the other hand, the model in the square tunnel has the same span-to-width ratio as the rectangular tunnel, but the model is 29% smaller in area. Another way to look at this is that, for the same size model as used in the square tunnel (diameter = 9.8 ft), a rectangular tunnel with an area of 262 ft² would give the same results. This would be a tunnel 19.8 × 13.2 ft for $W/H = 1.5$. Thus, the square tunnel has the excessive area that is indicated by the shaded portion on Fig. 12.

At the present time it appears that for a closed tunnel the most desirable shape is rectangular with a width-to-height ratio in the neighborhood of 1.5 without fillets. This tunnel can also, of course, be used as a rectangular tunnel with $W/H = 0.67$ by rotating the model 90°. If one does this using the same model size as the $W/H = 1.5$ tunnel (diameter = 11.7 ft), the allowable downwash can be increased 23% to 37°, and, of course, using a smaller model would allow testing still further into the transition region with a rectangular tunnel. It should also be noted that a future test series is planned using inserts with $W/H = 2.0$ to define more completely the question of the effect of tunnel geometry on this test limit for V/STOL vehicles.

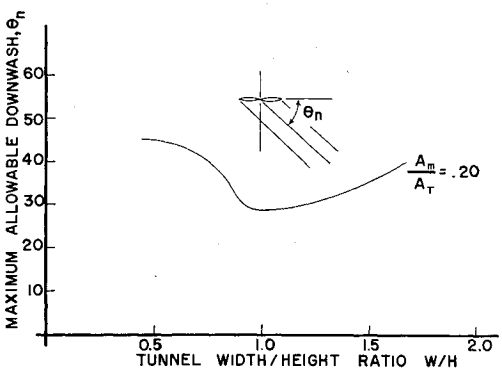

Fig. 10 Effect of tunnel geometry on maximum allowable downwash angles.

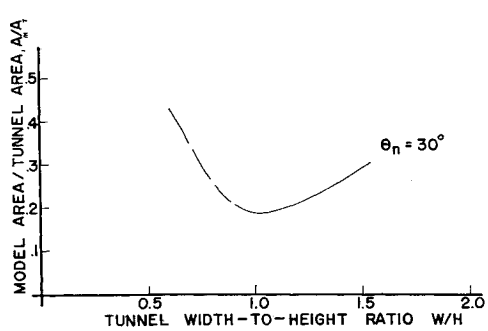

Fig. 11 Effect of tunnel geometry on model to tunnel area ratio.

The flow breakdown phenomenon is not the only limit that exists or must be considered in testing V/STOL models in wind tunnels. The flow breakdown limit only occurs when testing in the transition region where the model produces a flow with large downwash angles. Another factor that must be considered when determining the model size is the effect of wind-tunnel wall corrections. This factor applies throughout the whole speed range above the flow breakdown point. As pointed out in Ref. 4, the limitations on model size within a given wind tunnel are defined by the variation of the wall-induced interference over the model and not by the absolute size of the correction itself. The effect of changing the wind-tunnel width-to-height ratio on wall corrections both in regard to over-all magnitude and local distortion of the flow for V/STOL models can be determined by using the methods outlined in Refs. 3 and 4. Once the flow breakdown point has been reached, however, no wall correction theory will correct the data to free air, as the model is not being tested in a flow-field similar to free air.

There are, of course, other questions to be answered besides the effect of varying the tunnel width-to-height ratio on the flow breakdown. Some of these questions are as follows: How does the allowable downwash angle vary with fillet size for a given tunnel configuration? In this paper it was shown that the addition of large fillets, about 19% of the tunnel height for the 4- × 6-ft insert, reduces the model size by 22% for 30° downwash (Fig. 8). An analysis of data presented in Ref. 6 for a tilt wing model in a 7- × 10-ft wind tunnel gives a flow breakdown point that agrees quite well with the data presented in this paper for a tunnel without fillets. The 7- × 10-ft tunnel has, however, small fillets about 6 in. high and 9 ft long for lights. It may be that these small fillets either have no effect or such a small effect that they cannot be detected in the data. Based on present results, it appears that large fillets are not desirable. To find the minimum fillet that could be used would require a series of tests using a tunnel of fixed geometry with variable size fillets.

Another question is: How does the flow breakdown vary with model configuration? This is a most important and, at present, a most vexing question. If the flow breakdown is a function of the lift system and, hence, occurs at different downwash angles for rotors, lifting propellers, lift fans, jet flaps, and jet lift engines, then one is faced with the further question of whether or not variations within one type of lift system can affect the results. As mentioned previously, a tilt wing model with the whole wing behind the propellers gives results similar to those obtained with the rotor.[6] In Ref. 4, H. H. Heyson, at Langley Research Center, shows that similar results were encountered with a jet flap in a tunnel with $W/H = 0.70$. All of these models are similar in that the lift is distributed across the span, and they all give similar results in regard to the flow breakdown in the tunnel. When the tunnel flow breaks down with these models, the wake behind the model moves laterally across the floor and up the side walls, as shown in Fig. 13a.

The flow behind the model may be similar to Fig. 13b if the model does not have its lift distributed across the span similar to a rotor, but uses one of the following: a configuration similar to the XV-3 but with a large gap between the rotors, a ducted fan similar to the XV-22, lift fans similar to the VX-5A, or wing tip-mounted lift jets. This type of flow pattern may give a flow breakdown limit different from that discussed previously. It may also have a marked effect on the flow around the model in the region of the tail.

At The Boeing Co., W. M. Eldridge,[7] using a model with a tail and jet lift engines in the fuselage, shows that when this model encounters flow breakdown there is a sharp break in the curve of pitching moment vs the model normal force. Unpublished work at the University of Washington also has shown a similar effect on a tail-mounted 1-rotor-diam aft of the 2-ft rotor. In this work the zero lift angle of the tail is compared for the 8- × 12-ft tunnel and several inserts at various rotor

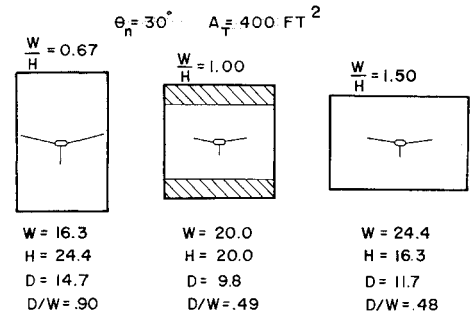

Fig. 12 Comparison of maximum-size rotor in different tunnels.

tip speed ratios for a constant shaft angle. The tail data in the inserts diverge from the 8- × 12-ft-tunnel data at lower downwash angles than that required for flow breakdown at the rotor; and when the rotor encounters flow breakdown there is a sharp break in the curve at the tail. From these data it appears that the tail is affected by flow breakdown before the rotor is affected. These experimental observations imply that even more severe limitations may be encountered by longitudinally distributed lift systems such as tandem rotors.

To answer fully the question of what effect the numerous proposed V/STOL configurations have upon wind-tunnel test limits due to flow breakdown will require many additional test programs. At the present time several programs are being undertaken at various facilities throughout the United States in an attempt to answer this question.

Another topic that should be discussed is in regard to possible fixes that might extend the downwash range of a given tunnel-model combination. There are at least four possible fixes that might be used. These are as follows: 1) the use of strakes on the tunnel floor to prevent the lateral flow of the model's wake across the floor; 2) the use of slots at the lower corners to prevent flow up the wall, or a slotted or false floor which will allow the model's wake to pass through; 3) some sort of boundary-layer control system on the floor and possibly the walls to carry downstream more rapidly the wake from the model; and 4) displacement of the model above the tunnel centerline.

Some unpublished test results from the University of Washington using various strake configurations have shown that strakes aft of a rotor will delay but not stop the breakdown of the flow in the tunnel. When strakes were added forward of the rotor the breakdown of the flow was more pronounced, and there was no gain in allowable downwash angle. The strakes may also have an effect on wall corrections which will be difficult to account for.

The use of slots on the tunnel walls will, of course, alter the wall corrections because of the porosity of the tunnel walls. At the present time there is, unfortunately, no theory available for wall corrections in slotted tunnels when the model produces large deflected wakes. A slotted tunnel may also require a very careful design of the plenum that surrounds the test section to prevent a recirculation-type flow forming in the plenum which then might feed back into the test section. A false floor is just another system of slotting the tunnel; and no floor, i.e., open on the bottom-tunnel, is one of the

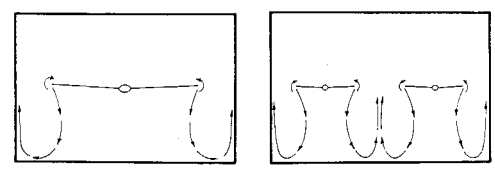

a) Single lift system b) Multiple lift systems

Fig. 13 Sketch of flow behind models in a closed wind tunnel.

poorest tunnel configurations from the standpoint of wall corrections.[3,4]

Since the flow breakdown occurs when the model's wake moves laterally across the tunnel floor to the walls, either a moving belt or a floor with blowing-type boundary-layer control system may aid in delaying the onset of flow breakdown. These systems would carry the model's wake downstream more rapidly and, thus, require the model to produce a higher downwash angle before the wake could reach the wall in the vicinity of the model. The use of a suction system on the floor to remove the model's wake may prove too difficult to achieve, as the wake location and mass flow will be a function of both the model's lift system and the flight condition that is being simulated.

Some preliminary work at the University of Washington using a 28.6- $\times$ 31.6-in. ($W/H = 1.1$) model tunnel has shown that raising the model above the center line tends to increase the allowable downwash angle. Heyson, in some unpublished work at Langley Research Center, has shown similar results using a jet-flap model. Turner[8] also indicates that an increase in model height above the ground reduces the need for a moving belt to prevent a flow breakdown. There must be, however, some limit in regard to raising the model above the centerline, because eventually the ceiling will constrain the inflow into the model.

Some unpublished results from Langley Research Center using a tunnel with a floor only and a jet-flap model have shown a loss in lift from free air data similar to that obtained in a closed tunnel, although this lift loss occurred at slightly higher downwash angles. Turner,[8] in a paper dealing with ground effect testing over a moving belt, shows that when testing over a fixed ground board there is a larger loss of lift than that obtained with a moving model or moving belt. This lift loss near the ground apparently is caused by a flow phenomenon similar to that encountered in the tunnel with a floor only. Thus, there appear to be two distinct types of flow breakdown. One is caused by the wake from the model moving across the floor laterally and then up the tunnel walls, and the second one is caused by the wake moving forward along the floor under the model. It is apparent that both types of flow breakdown occur to varying degrees when testing in closed throat wind tunnels. The lateral type of flow breakdown based on present results affects the model at lower downwash angles than the forward type. However, both types result in a loss of lift at the model.

At the present time none of these questions can be completely answered. They do, however, point out not only areas that need future investigation but also areas where the unwary may get into serious trouble when testing V/STOL aircraft in either research or developmental test programs.

Conclusions

This study of testing limits for V/STOL vehicles indicates the following conclusions.

1) For any closed-throat wind tunnel that is used for V/STOL testing, there is a definite test limit at low forward speeds. This test limit is caused by a breakdown of the flow in the wind tunnel which results in a flow past the model that does not simulate the flow encountered by the vehicle in free air.

2) The test limits caused by flow breakdown are a function of the geometry of the wind tunnel. For a given tunnel configuration, the limit is a function of the model size. The use of fillets in all tunnel configurations reduces the allowable downwash angles, and thus fillets should be avoided.

3) At present, the optimum tunnel configuration appears to be a rectangular tunnel that is wider than it is high with no fillets. Such a tunnel is superior to a square tunnel as it allows the use of a larger model for a given tunnel cross-section area. This tunnel configuration has the additional advantage of allowing the model to be rotated 90° so that tests with the same size or a smaller model can be conducted in a narrow, deep tunnel at higher downwash angles.

References

[1] Ganzer, V. M. and Rae, W. H., Jr., "An experimental investigation of the effect of wind tunnel walls on the aerodynamic performance of a helicopter rotor," NASA TN D-415 (1960).

[2] Lee, J. L., "An experimental investigation of the use of test section inserts as a device to verify theoretical wall corrections for a lifting rotor centered in a closed rectangular test section," Masters Thesis, Dept. of Aeronautics and Astronautics, Univ. of Washington (1964).

[3] Heyson, H. H., "Linearized theory of wind tunnel jet boundary corrections and ground effect for VTOL-STOL aircraft," NASA TR R-124 (1962).

[4] Heyson, H. H. and Grunwald, K. J., "Wind tunnel boundary interference for V/STOL testing," Conference on V/STOL and STOL Aircraft, Paper 24, NASA SP-116 (1966).

[5] Heyson, H. H., "Nomographic solution of the momentum equation for VTOL-STOL Aircraft," NASA TN D-814 (1961).

[6] Grunwald, K. J., "Experimental study of wind tunnel wall effects and wall corrections for a general research V/STOL tilt-wing model with flap," NASA TN D-2887 (1965).

[7] Eldridge, W. M. "An evaluation of wall interference effects and test limits for a jet-lift V/STOL wind tunnel model," The Boeing Company, Airplane Div., D6-15021TN (1966).

[8] Turner, T. R., "Endless-belt technique for ground simulation," Conference on V/STOL and STOL Aircraft, Paper 25, NASA SP-116 (1966).